

Flux creep in type-II superconductors: The self-organized criticality approach

R. G. Mints* and Ilya Papiashvili

School of Physics and Astronomy, Raymond and Beverly Sackler Faculty of Exact Sciences, Tel Aviv University, Tel Aviv 69978, Israel

(Received 24 October 2004; revised manuscript received 17 March 2005; published 25 May 2005)

We consider the current density distribution function of a flux-creep regime in type-II superconductors by mapping flux creep to a model with a self-organized criticality. We use an extremal equal-redistribution-type model which evolves to Bean's state, to treat magnetic flux penetration into superconductors and derive analog of current-voltage characteristics in the flux-creep region.

DOI: 10.1103/PhysRevB.71.174509

PACS number(s): 74.25.Ha

I. INTRODUCTION

In the presence of transport currents, the vortex structure in a type-II superconductor is subjected to the Lorentz force. This force per unit length of a vortex is $\mathbf{f}_L = \mathbf{j} \times \vec{\phi}_0$, where \mathbf{j} is the transport current density, $\vec{\phi}_0 = \phi_0 \mathbf{B}/B$, \mathbf{B} is the magnetic induction, and ϕ_0 is the flux quantum. The Lorentz force acting on a unit volume of a vortex matter is therefore given by $\mathbf{F}_L = n \mathbf{f}_L = \mathbf{j} \times \mathbf{B}$, where $n(\mathbf{r}) = B(\mathbf{r})/\phi_0$ is the density of the vortices.^{1,2}

Consider as an illustration a superconducting slab parallel to the y, z plane and assume that a certain magnetic field B_a is applied along the z axis as shown in Fig. 1. In this case, we have $\mathbf{j} = j\hat{y}$ and $\mathbf{B} = B\hat{z}$ related by Maxwell's equation $dB/dx = -\mu_0 j$. The Lorentz force $F_L = jB$ is therefore proportional to the density of vortices n and its gradient dn/dx as follows from $F_L = jB \propto B dB/dx \propto n dn/dx$.

In high-current-density superconductors, defects of the crystalline structure "pin" vortices. This leads to the creation of various vortex configurations with flux "hills" and flux "valleys." Indeed, single vortices or vortex bundles redistribute spatially if the Lorentz force $F_L \propto j \propto dn/dx$ overcomes the pinning force F_{pin} . This means that $n dn/dx \propto F_{\text{pin}}$, i.e., a steady vortex structure consists of fragments with slopes $dn/dx \neq 0$ (flux hills). On a macroscopic level, we have $F_L \propto j$ and, therefore, the local depinning of vortices happens when the local current density j exceeds a certain critical value $j_c \propto F_{\text{pin}}$. It was pointed out by de Gennes that the flux hills with slopes statistically fixed by the critical current density j_c are very much like sand piles.¹

An effective approach to flux statics and dynamics in superconductors with a high density of pinning centers was first suggested by Bean.³ The famous Bean model assumes that the current density j is equal to the critical current density j_c anywhere through the current carrying region. Originally, Bean considered the magnetic field independent j_c . As a result, the spatial variation of the field inside the sample is linear, e.g., in a slab with thickness $2d$ (see Fig. 1), $j_c = \text{constant}$ leads to $B = B_a - \mu_0 j_c |x \mp d|$, where B_a is the field at the sample surface. In general, for a better description of the data available, the field dependence of j_c has to be taken into account.^{4,5}

In this paper, we treat the low-temperature flux creep in type-II superconductors in the framework of the self-organized criticality.⁶⁻¹⁷ We perform numerical simulations

in terms of current density j , i.e., on a "macroscopic" level and assume that the rules of dynamics of j are formed on a "microscopic" level of vortex avalanches.⁸ The distribution function $G(j)$ of the current density j is considered for an equal-redistribution-type process.⁹ We show that this process results in a self-organized Bean's state with a complex dynamics, which can be mapped onto the low-temperature flux creep.

The paper is organized as follows. In Sec. II, we discuss the low-temperature flux creep. The self-organized criticality of extremal process is treated in Sec. III. In Sec. IV, we introduce the low-temperature flux-creep model and derive the distribution function of the current density j . The magnetic flux penetration into type-II superconductors and an analog of current-voltage characteristics in the flux creep regime are discussed in Sec. V. Section VI summarizes the obtained results.

II. FLUX CREEP IN SUPERCONDUCTORS

There are few mechanisms which cause the depinning of vortices for currents with a density less than the critical value. In particular, both thermally activated depinning and quantum tunneling^{4,18} result in vortices or vortex bundles jumping from one group of pinning centers to another. This type of vortex motion is called flux creep.¹⁹ It is observed if the current density is from a narrow vicinity of the critical current ($|j - j_c| \ll j_c$). The probability of depinning of a vortex bundle depends strongly on the current density and tends to unity when $j \rightarrow j_c$. The strong intervortex interaction leads to

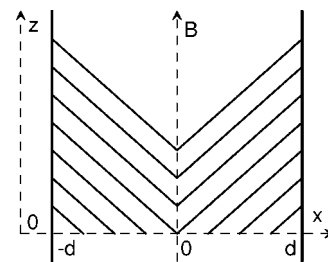


FIG. 1. Series of Bean's states in a slab parallel to the yz plane. A zero-field-cooled sample was subjected to a monotonically increased field parallel to the z axis. The slope of $B(x)$ is proportional to the critical current density j_c .

a very complicated collective behavior of the vortex matter especially in thin films where the stray fields result in non-locality of the problem.²⁰ Activation of a single vortex can launch a local avalanche-type motion of vortex bundles, i.e., in the flux-creep region, the vortex matter is a system with avalanche-driven dynamics. Such systems are the subject of the modern theory of self-organized criticality which revealed a variety of power-law distributions for the size and duration of avalanches.^{6,7}

Motion of vortices is accompanied by dissipation of energy. This can heat up the whole sample or a part of it to a temperature higher than the critical temperature T_c . Under certain conditions, an avalanche of even a small group of vortices can trigger a run-away magnetothermal instability causing the superconducting-to-normal transition.²¹

Within the original Bean model, the dependence of j on the electric field E is a highly nonlinear stepwise function

$$\mathbf{j} = \mathbf{j}_c \begin{cases} 0, & \text{if } E = 0, \\ 1, & \text{if } E \neq 0, \end{cases} \quad (1)$$

where $\mathbf{j}_c = j_c \mathbf{E}/E$ and the electric field \mathbf{E} is induced by the flux motion.

It is well established now that in the narrow vicinity of the critical current ($|j - j_c| \ll j_c$), i.e., in the flux-creep regime, the dependence of $E(j)$ is a very steep function given by the power law

$$\mathbf{j} = \mathbf{j}_c \left(\frac{E}{E_0} \right)^{1/n}, \quad (2)$$

where $n \gg 1$ is a parameter and E_0 defines the critical current density. It is common to define j_c as the current density at $E_0 = 10^{-6}$ V cm⁻¹. It is worth mentioning that for $n \gg 1$ we can rewrite Eq. (2) as

$$\mathbf{j} = \mathbf{j}_c + \frac{\mathbf{j}_c}{n} \ln \left(\frac{E}{E_0} \right), \quad (3)$$

where the omitted terms are of the order $1/n^2 \ll 1$.

Equation (2) was first derived considering the thermally activated uncorrelated hopping of vortex bundles, the Anderson–Kim model.⁵ The vortex-glass²² and collective creep^{23,24} models suggested later result in more sophisticated dependencies of j on E . Still, these dependencies reduce to Eq. (2) provided $j - j_c \ll j_c$. The recently developed approach of the self-organized criticality^{11,12} also leads to Eq. (2) if $j - j_c \ll j_c$. It should be stressed that in the interval $j - j_c \ll j_c$, the power law (2) is in good agreement with numerous experimental data.²⁵

A detailed study of the vortex dynamics in the flux-creep regime was performed by Field and co-workers.¹³ In their experiments, the magnetic field outside a tubular superconducting sample is ramped slowly, driving the flux into the tube outer wall. After the flux front reaches the inner wall, it spills out into the tube interior, the process recorded in real time. This experiment distinguished between flux leaving the superconductor in discrete bundles or avalanches. It was shown that the probability $\mathcal{D}(s)$ of an avalanche containing s vortices is a power law extending over 1.6 decades.

The dynamics of Bean’s state is typical of other spatially extended dynamical systems. The high number of degrees of freedom in these systems introduces the problem of coupling between the individual degrees of freedom. In many cases, even very complicated systems “self-organize” so that their behavior can be described by a small number of collective degrees of freedom.^{6,7}

In some dynamical systems, individual degrees of freedom keep each other in a stable balance, which is not a “perturbation” of some decoupled state and the situation cannot be described in terms of a small number of collective degrees of freedom. This type of the self-organized systems has to be quite robust, otherwise, these systems would not be able to evolve to a stable balanced “critical” state.^{6,7} The sand piles and flux hills in superconductors exhibit many features typical for the self-organized critical state.

Several models were suggested to study dynamical systems with extended spatial degrees of freedom and many metastable states. These systems evolve to a *self-organized* critical state without a detailed specification of the initial conditions, i.e., the critical state is an *attractor*—robust with respect to variations of parameters and the presence of quenched randomness.

III. SELF-ORGANIZED CRITICALITY OF EXTREMAL PROCESSES

We consider now a specific subclass of *extremal* processes demonstrating the self-organized criticality. In extremal models, only the sites satisfying a certain extremal criterion are involved at each step of the system evolution. In particular, the problem of low-temperature flux creep in superconductors can be mapped onto an extremal model.^{9,10}

A. Low-temperature flux-creep model

At low temperatures, vortices at sites with slightly different current densities have a different probability of depinning: The depinning will happen first in a site with the highest current density.

The model suggested by Zaitsev⁹ simulates a part of a superconductor with L sites using the closed boundary conditions. Numbers j_i ($0 \leq i \leq L$) are the values of the current density j_y at L sites of the x axis. At each simulation step, a site number m with the maximum current density j_m is found (see Fig. 2). This current density is reduced by a certain value Δ chosen randomly with an equal probability from the interval $0 < \Delta < 1$:

$$j_m \rightarrow j_m - \Delta, \quad j_{m \pm 1} \rightarrow j_{m \pm 1} + \Delta/2. \quad (4)$$

It was shown that the stationary state of this model exhibits the basic features typical for self-organized criticality systems.⁹ It is worth mentioning that Zaitsev’s model conserves the total current

$$I = \sum_{n=1}^L j_n = \langle j \rangle L, \quad (5)$$

so that the average current density $\langle j \rangle$ is also conserved.

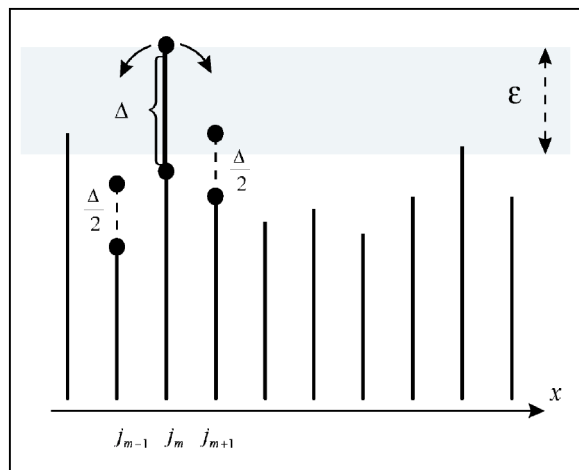


FIG. 2. Illustration of the dynamics rules of Zaitsev's low-temperature flux-creep model.

The system approaches Bean's state starting from any initial state with a given $\langle j \rangle$. In this state, almost all sites have current densities less than a certain value j_c . We assume that each site maps an area in a superconductor containing a bundle of vortices and ascribe the depinning of this bundle to a single "vortex" of Zaitsev's model. Motion of this vortex changes the local current density by Δ . The distribution of the values of Δ (referred to below as Δ -distribution) is related to the amount of vortices leaving a given site, i.e., all details concerning vortex dynamics, including microscopic vortex dynamics, are "hidden" in the Δ -distribution.

B. Dynamics of extremal processes

The flux-creep model described above conserves the total current I ; this leads to a high level of correlation between the sites. In extremal models, the extremal sites are chosen according to problem-specific criteria. We will call these sites *ignition* sites. The changes at ignition sites provoke changes at neighboring sites, again according to rules specific for a given model. The sites drawn to be active by the ignition sites will be called *involved*. An involved site in its order can become an ignition site if it matches a certain extremal criterion. A system in a critical state is characterized by a critical value of some dynamic parameter. For the flux-creep model, this parameter is j_c which is the *least* value of j in the ignition sites. That means that for the flux-creep model, all ignition sites have values greater than j_c .

The rules of dynamics given by Eq. (4) are illustrated schematically in Fig. 3. The interval of values of current densities at ignition sites is called an *active zone*. Each site in the active zone, an *active* site, becomes an ignition site at a certain moment. At any step, only a small part of all sites is active. As shown in Fig. 3, the majority of sites belongs to the *calm zone*. We will consider the dynamic properties of the low-temperature creep model (4) using this terminology.

IV. LOW-TEMPERATURE CREEP SIMULATIONS

We have performed numerical simulations of the low-temperature flux creep based on the rules of dynamics given

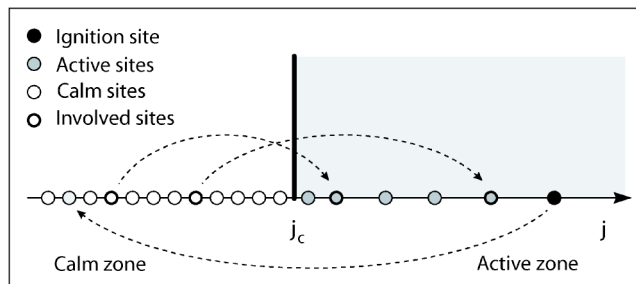


FIG. 3. The calm and the active zones for a one-dimensional flux creep model. The rules of dynamics given by Eq. (4) are illustrated by the dashed lines.

by Eq. (4). Our simulations clearly demonstrate that the current density distribution $G(j)$ is an exponential dependence up to a certain critical value j_c , i.e.,

$$G(j) = A \exp(j/j_e), \quad \text{for } j_c - 1 < j < j_c, \quad (6)$$

where A and j_e are parameters of the distribution (see Fig. 4). The distribution function $G(j)$ is cut off sharply at $j=j_c$. In the active zone ($j > j_c$) the "tail" of $G(j)$ decreases as $1/L$, when $L \rightarrow \infty$ (see Fig. 5).

The function $G(j)$ has another cutoff at $j_c - 1$ if the Δ -distribution in the interval $(0,1)$ is chosen to be uniform. Indeed, there are only two options to have a site with the current density j : (a) To decrease the current density in the ignition site by Δ , and (b) to increase the current density in one of the involved sites by $\Delta/2$. The lowest value of j is obtained by subtracting from the minimum value of the current density in an ignition site, which is j_c , the maximum value from the Δ -distribution, which is 1. As a result, the distribution function $G(j)$ has a cutoff from the left. This cutoff is not universal and depends on the Δ -distribution. A continuously decreasing Δ -distribution eliminates both the left cutoff and the deviation of $G(j)$ from the exponential in the vicinity of j_c . The details of the Δ -distribution affect only the tail of the function $G(j)$ in the interval $j > j_c$. Therefore, values of the current density j are distributed according to the exponential law of Eq. (6) in almost all sites of the system.

A. Relation between the currents j_e and j_c

This relation can be calculated analytically using the normalization of the distribution function $G(j)$ and the average current density conservation rules. Indeed, the normalization

$$\int_{-\infty}^{j_c} G(j) dj = A \int_{-\infty}^{j_c} \exp(j/j_e) dj = 1 \quad (7)$$

relates A , j_c , and j_e

$$A = \frac{1}{j_e} \exp(-j_c/j_e). \quad (8)$$

Next, we calculate the average value of the current density

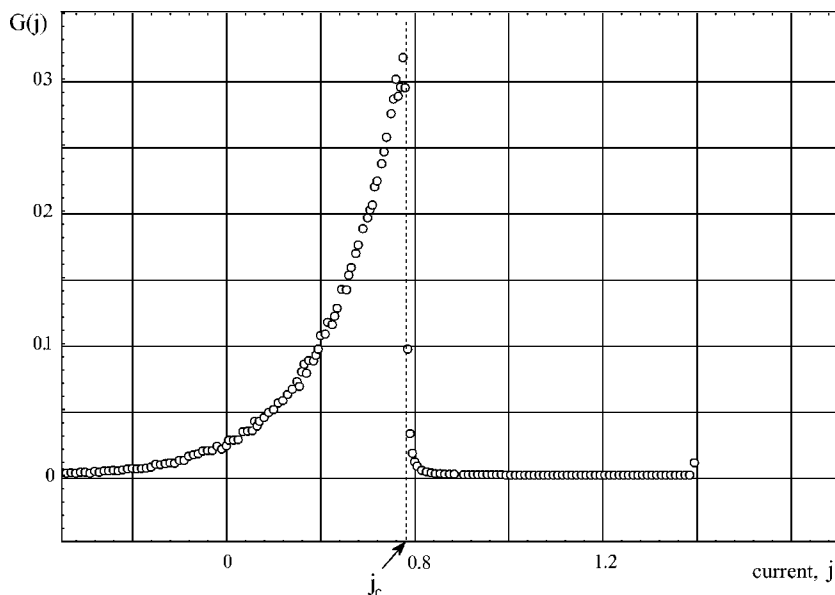


FIG. 4. The dependence of the distribution function $G(j)$ on the current density j .

$$\langle j \rangle = \int_{-\infty}^{j_c} jG(j) dj \quad (9)$$

and obtain the relation of A , j_c , and j_e to $\langle j \rangle$:

$$\langle j \rangle = Aj_e^2(j_c/j_e - 1)\exp(j_c/j_e). \quad (10)$$

Combining Eqs. (8) and (10), we find:

$$j_c - j_e = \langle j \rangle. \quad (11)$$

If the Δ -distribution is uniform, we have $\langle j \rangle = 1/2$ and

$$j_c - j_e = 1/2. \quad (12)$$

B. Origin of the exponential dependence $G(j)$

We performed numerical simulations for a few different extremal models and obtained the current density distribution function $G(j)$ for all of them. In addition to the uniform distribution for Δ , we tested exponential, Gaussian, and power-law distributions. These Δ -distributions are more “natural” than the uniform Δ -distribution, since they decay gradually and have no cutoffs. All of them lead to the exponential form of $G(j)$ if two conditions are satisfied: (1) Interactions in the model are local, meaning that an ignition site affects only sites in a nearby region of a finite size, and (2) at each step, the sum of dynamical variables (j_i) stays constant. In other words, the exponential form (6) of $G(j)$ is universal; meaning that it does not depend on the form of the Δ -distribution, on the dynamic rules of redistribution of Δ between neighbors, and on how many sites from the vicinity of an ignition site are involved in the redistribution process (for example, next-nearest neighbors can be included into the dynamics). Thus, the exponential behavior of $G(j)$ is typical for extremal models with short-range interactions and a conservation relation for the dynamical variable.

The exponential behavior of $G(j)$ can be obtained analytically as the most probable distribution of the dynamical vari-

able j_i . To simplify the derivation, we use discrete values of j by dividing the domain of possible values of j into small intervals. In this case, each site is characterized by a certain value j_i . We denote the number of sites with the same value j_i as n_i and write the conservation relations in the form

$$\sum_i n_i = L, \quad \sum_i n_i j_i = \langle j_i \rangle L. \quad (13)$$

Distribution of L sites among the intervals with $j = j_i$ is described by a set $\{n_i\}$, where n_i is a number of sites in each interval. The number of states corresponding to the same set $\{n_i\}$ is given by

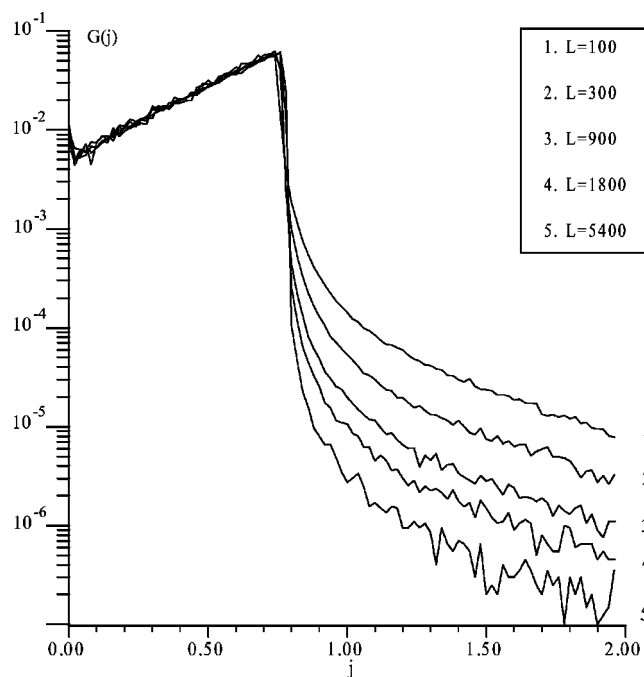


FIG. 5. Distribution functions $G(j)$ for different values of the length of the system L in the region $j > j_c$ [tails of $G(j)$].

$$\Gamma = \frac{L!}{\prod_i n_i!}. \quad (14)$$

Using Stirling's formula, we have for $\sigma = \ln \Gamma$

$$\sigma = L \ln L - \sum_i n_i \ln n_i \quad (15)$$

The maximum of σ is found using Lagrange method for conditional extremum with two conditions (13)

$$F = \sigma + (\alpha + 1)L - \beta \langle j \rangle L, \quad (16)$$

$$\frac{\partial F}{\partial n_i} = -\ln n_i + \alpha + \beta j_i = 0.$$

We finally obtain

$$n_i = e^{\alpha + \beta j_i} \quad (17)$$

with α and β defined by

$$\sum_i e^{\alpha + \beta j_i} = L, \quad \sum_i j_i e^{\alpha + \beta j_i} = \langle j \rangle L. \quad (18)$$

Using continuous forms of Eq. (18)

$$\int e^{\alpha + \beta j} dj = L, \quad \int j e^{\alpha + \beta j} dj = \langle j \rangle L, \quad (19)$$

we find

$$\beta = \frac{1}{j_e}, \quad e^\alpha = A = \frac{1}{j_e} \exp\left(-\frac{j_c}{j_e}\right). \quad (20)$$

Thus, j_c , j_e , and $\langle j \rangle$ are indeed related by Eq. (11) and

$$G(j) = \frac{1}{j_e} \exp\left(\frac{j - j_c}{j_e}\right) = \frac{1}{e j_e} \exp\left(\frac{j - \langle j \rangle}{j_e}\right). \quad (21)$$

This distribution function contains an independent parameter j_e characterizing the function width. The value of j_e is proportional to the width $\delta\Delta$ of the Δ -distribution and depends on the spatial dimension of the model, on the number of the neighbors of the ignition site, etc.

It is worth mentioning that the main features of the distribution function $G(j)$ can be formulated in terms of a certain effective "temperature." Indeed, the above derivation of $G(j)$ is based on the arguments which are used to derive the Gibbs distribution for a system of nonidentical particles. We can rewrite Eq. (21) in the form $G(j) = \exp(-\epsilon_j/\tau)/j_e$, where the effective "energy" ϵ_j and the "temperature" τ are defined as $\epsilon_j = a(j_c - j)$ with an arbitrary coefficient a and $\tau = a j_e$. Using Eq. (11), we find for the average energy

$$\langle \epsilon_j \rangle = a(j_c - \langle j \rangle) = a j_e = \tau. \quad (22)$$

The parameter j_e is proportional to the width $\delta\Delta$ of the Δ -distribution, and the same is true for the effective temperature: $\tau \propto \delta\Delta$.

V. FLUX PENETRATION MODEL

Extremal models are useful for studying macroscopic processes in superconductors and, in particular, the magnetic

flux penetration. The periodic boundary conditions which we used above were convenient to describe the part of the system far from the sample edges. In this section, we modify the model to allow for studying the flux penetration.

Consider a slab in the parallel magnetic field as shown in Fig. 1. Due to the symmetry, we can do simulations in one-half of the sample. Assume that the applied field increases with a rate \dot{h} and penetrates the sample from the edge at $x = -d$. At this edge, we have:

$$j_0(t + \delta t) = j_0(t) + \dot{h} \delta t. \quad (23)$$

The dynamics rule at the middle of the slab ($x=0$) has the form

$$j_L(t + \delta t) = j_L(t) - \Delta,$$

$$j_{L-1}(t + \delta t) = j_{L-1}(t) + \Delta/2, \quad (24)$$

where $j_L(t)$ corresponds to the site at $x=0$. It is worth mentioning that there is no current conservation at the sample boundaries at each simulation step. However, in a stationary state, the current conservation holds for large time intervals.

A. Introduction of the "real" time scale

The above model of the self-organized low-temperature flux creep does not formulate the rules of the current density dynamics in terms of real time; instead, it operates with the simulation steps. These steps correspond to the sequential depinning events in the process of numerical simulation. The real time step corresponding to two successive simulation steps depends on temperature, current density, and other parameters of the system, and can vary significantly. This has to be taken into account in order to relate the numerical and experimental data.

The temporal variation of the applied magnetic field has its time scale, which has to be synchronized with the "inner clock" of numerical simulations. This synchronization can be done by calculating the real time interval between two successive depinning events. The extremal models of the low-temperature creep are based on the assumption that the depinning probability P_d strongly depends on the maximum current j_m . We assume that this dependence has the exponential form

$$P_d \propto \exp\left[\frac{j_m - j_c}{j_1}\right] \propto \exp\left[\frac{j_m}{j_1}\right], \quad \text{for } j_m < j_c. \quad (25)$$

The mean time between two depinning events $\langle \delta t \rangle$ is inversely proportional to P_d and, therefore, we write

$$\langle \delta t \rangle = \delta t_r \exp\left[-\frac{j_m(t)}{j_1}\right], \quad (26)$$

where δt_r is the time interval of a *tick* of the "real clock." The last equation provides the synchronization rule for the numerical steps.

Using Eqs. (23) and (26), we arrive at the synchronized boundary condition at $x = -d$ in the form

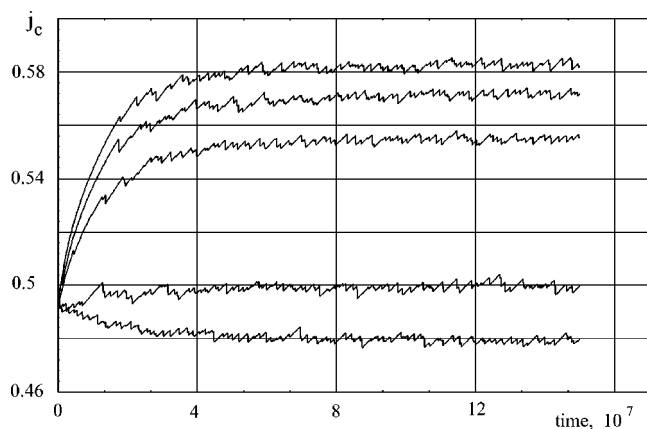


FIG. 6. Starting from the same initial distribution, the current density approaches different asymptotic values depending on the ramp rate $\dot{h}=4 \times 10^{-5}$, 3×10^{-5} , 2×10^{-5} , 5×10^{-6} , and 3×10^{-6} (from top to bottom).

$$j_0(t + \delta t) = j_0(t) + \dot{h} \delta t_r \exp\left[-\frac{j_m(t)}{j_1}\right]. \quad (27)$$

Changing the time scale so that $\dot{h} \delta t_r \rightarrow \dot{h}$, we rewrite Eq. (27) in the form convenient for recursive calculations

$$j_0 \rightarrow j_0 + \dot{h} \exp\left[-\frac{j_m}{j_1}\right]. \quad (28)$$

We now treat the numerical analog of the j - E curve for the low-temperature magnetic flux creep. The self-organized criticality model does not operate with the electric field E explicitly. Therefore, we have to relate the field E to certain characteristics of the model.

When a stable state is established, the magnetic flux redistributes inside the sample keeping the critical current density j_c almost constant. According to the Faraday law, the magnetic field varying in time generates an electrical field. We assume here that the dependence between E and \dot{h} is linear, i.e., $E \propto \dot{h}$.

We demonstrate in Fig. 6 how the asymptotic current density j is established for several values of the magnetic field ramp rate \dot{h} . Figure 7 shows the dependence of E on the

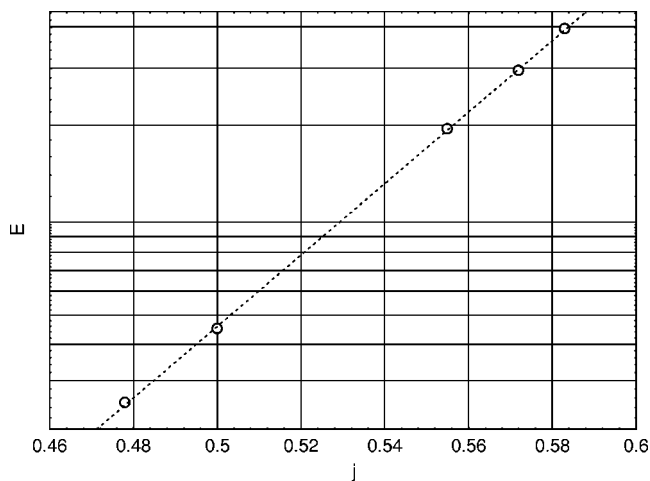


FIG. 7. Analogue of the current-voltage characteristics.

asymptotic value of j , the analog of the j - E curve of Bean's state. This logarithmic j - E curve is consistent with Eq. (3) as well as with numerous experimental data.²⁵

VI. SUMMARY

We demonstrate that an extremal type model evolves to Bean's type state. The distribution function of the current density $G(j)$ in this self-organized state was obtained by numerical simulations as well as analytically. We found that $G(j)$ has a characteristic cutoff at the critical current density. We map the low-temperature magnetic flux-creep process to dynamics of an extremal model with Bean's type critical state to treat magnetic flux penetration into superconductors and derive an analog of the current-voltage characteristics in the flux creep regime.

ACKNOWLEDGMENTS

One of us (R.G.M.) is grateful to V. G. Kogan for useful discussions and stimulating criticisms. This research was supported by The Israeli Science Foundation (Grant No. 283/00-11.7).

*Electronic mail: mints@post.tau.ac.il

¹P. G. de Gennes, *Superconductivity of Metals and Alloys* (W. A. Benjamin, New York, 1966).

²A. M. Campbell and J. E. Ivett, *Critical Currents in Superconductors* (Taylor and Francis, London, 1972).

³C. P. Bean, *Phys. Rev. Lett.* **8**, 250 (1962).

⁴P. W. Anderson, *Phys. Rev. Lett.* **9**, 309 (1962).

⁵P. W. Anderson and Y. B. Kim, *Rev. Mod. Phys.* **36**, 39 (1964).

⁶P. Bak, *How Nature Works—The Science of Self-Organized Criticality* (Copernicus, New York, 1996).

⁷H. J. Jensen, *Self-Organized Criticality—Emergent Complex Be-*

haviour in Physical and Biological Systems (Cambridge University Press, Cambridge, UK, 1998).

⁸E. Altshuler and T. H. Johansen, *Rev. Mod. Phys.* **76**, 471 (2004).

⁹S. I. Zaitsev, *Physica A* **189**, 411 (1992).

¹⁰A. S. Datta, K. Christensen, and H. J. Jensen, *Europhys. Lett.* **50**, 162 (2000).

¹¹Z. Wang and D. Shi, *Solid State Commun.* **90**, 405 (1994).

¹²W. Pan and S. Doniach, *Phys. Rev. B* **49**, 1192 (1994).

¹³S. Field, J. Witt, F. Nori, and X. Ling, *Phys. Rev. Lett.* **74**, 1206 (1995).

¹⁴C. M. Aegerter, *Phys. Rev. E* **58**, 1438 (1998).

- ¹⁵K. Behnia, C. Capan, D. Maily, and B. Etienne, *Phys. Rev. B* **61**, R3815 (2000).
- ¹⁶M. Nicodemi and H. J. Jensen, *Phys. Rev. Lett.* **86**, 4378 (2001).
- ¹⁷C. M. Aegerter, M. S. Welling, and R. J. Wijngaarden, *Europhys. Lett.* **65**, 753 (2004).
- ¹⁸L. I. Glazman and N. Y. Fogel, *Fiz. Nizk. Temp.* **10**, 95 (1984) [*Sov. J. Low Temp. Phys.* **10**, 51 (1984)].
- ¹⁹M. R. Beasley, R. Labusch, and W. W. Webb, *Phys. Rev.* **181**, 682 (1969).
- ²⁰I. S. Aranson, A. Gurevich, M. S. Welling, R. J. Wijngaarden, V. K. Vlasko-Vlasov, V. M. Vinokur, and U. Welp, *Phys. Rev. Lett.* **94**, 037002 (2005).
- ²¹R. G. Mints and A. L. Rakhmanov, *Rev. Mod. Phys.* **53**, 551 (1981).
- ²²H. Eskes and G. A. Sawatzky, *Phys. Rev. Lett.* **61**, 1415 (1988).
- ²³A. I. Larkin and Y. N. Ovchinnikov, *Zh. Eksp. Teor. Fiz.* **65**, 1704 (1973) [*Sov. Phys. JETP* **38**, 854 (1973)].
- ²⁴M. V. Feigelman, V. B. Geshkenbein, A. I. Larkin, and V. M. Vinokur, *Phys. Rev. Lett.* **63**, 2303 (1989).
- ²⁵See A. Gurevich and H. K pfer, *Phys. Rev. B* **48**, 6477 (1993) and the references therein.